A theoretical study of tunneling conductance in PrOs$_4$Sb$_{12}$ superconducting junctions

Yasuhiro Asano*

Department of Applied Physics, Hokkaido University, Sapporo 060-8628, Japan

Yukio Tanaka

Department of Applied Physics, Nagoya University, Nagoya 464-8603, Japan

Yuji Matsuda

Institute for Solid State Physics, University of Tokyo, Kashiwa, Chiba 277-8581, Japan

Satoshi Kashiwaya

National Institute of Advanced Industrial Science and Technology, Tsukuba 305-8568, Japan

The tunnel conductance in normal-metal/insulator/ProS$_4$Sb$_{12}$ junctions is theoretically studied, where skutterudite ProS$_4$Sb$_{12}$ is considered to be an unconventional superconductor. The conductance is calculated for several pair potentials which have been proposed in recent work. The results show that the conductance is sensitive to the relation between the direction of electric currents and the position of point nodes. The conductance spectra often deviate from the shape of bulk density of states. The sub gap spectra have peak structures in the case of the spin-triplet pair potentials. The results indicate that the tunnel conductance is a useful tool to obtain information of the pairing symmetry.

I. INTRODUCTION

Superconductivity in cubic skutterudite PrOs$_4$Sb$_{12}$ (POS) has received much interest in recent years since it has two superconducting phases.[1] The specific heat results[2] show jumps at $T_{c1} = 1.82$ K and $T_{c2} = 1.75$ K. Nowadays two such superconducting phases are well known in a spin-triplet superconductor UPt$_3$ and a superfluid ^{3}He. A NQR experiment shows the absence of the coherence peak, which suggests that POS is an unconventional superconductor.[3] A thermal conductivity experiment indicates six point nodes at (1,0,0) direction and directions equivalent to (1,0,0) for the high-temperature phase (H phase)[4].

The mechanism and the symmetry of pairing have been discussed in several theoretical studies.[5–9] POS should be distinguished from the other unconventional superconductors, in that it has a nonmagnetic ground state of the localized f electrons in the crystalline electric field. The origin of heavy Fermion behavior in this compound has been discussed in terms of the interaction of the electric quadrupole moments of Pr^{3+} with the conduction electrons, rather than local magnetic moments as in the other heavy Fermion superconductors. Therefore the relation between the superconductivity and the orbital fluctuation of f electron state has aroused great interest; POS is a candidate for the first superconductor mediated neither by electron-phonon nor magnetic interactions. Hence it is of the utmost importance to determine the symmetry of the superconducting gap. At present, however, the pairing symmetry of POS is still unclear. This is simply because we lack both experimental data and theoretical analysis enough to address the pairing symmetry. So far, a possibility of anisotropic s wave symmetries has been discussed for spin-singlet Cooper pairs. In the low-temperature phase (L phase), an additional symmetry break-

ing decreases the number of point nodes to 4 or 2.[9,6] The spin-triplet superconductivity still has a possibility,[7] where the pairing interaction is mediated by the quadrupolar fluctuations. The double transition is more easily constructed in spin-triplet pairing with degeneracy due to the time-reversal symmetry than the spin-singlet pairing.[7] In a theory,[5] unitary and nonunitary spin-triplet states are proposed for H and L phases, respectively.

Generally speaking, the tunneling spectra are expected to reflect the bulk density of states (DOS) of superconductors. This is true for isotropic s wave superconductors. In unconventional superconductors, however, the tunneling spectra often differ from the bulk DOS. A zero-bias conductance peak (ZBCP) of high-T_c materials is an important example.[10–18] The interference effect of a quasiparticle enables the zero-energy Andreev bound states on the Fermi energy at surfaces of d wave superconductors.[19,20] The formation of the zero-energy states (ZES's) is a universal phenomenon expected in unconventional superconductors,[11,21–25] and affects the low-temperature behavior of charge transport properties[26–30] and the Josephson current.[31–44] When the direction of the electric current deviates from the a axis of high-T_c superconductors, a large conductance peak is observed around the zero bias, which reflects the DOS of such surface states. When the current is parallel to the a axis, on the other hand, the conductance shape is close to that of the bulk DOS in high-T_c superconductors. Thus the tunneling spectra are essentially anisotropic in unconventional superconductors, which means that it is possible to extract useful information of the pairing symmetry from tunneling spectra.

The purpose of this paper is to demonstrate the differential conductance in normal-metal/insulator/POS junctions for several pair potentials proposed in recent studies. The junc-
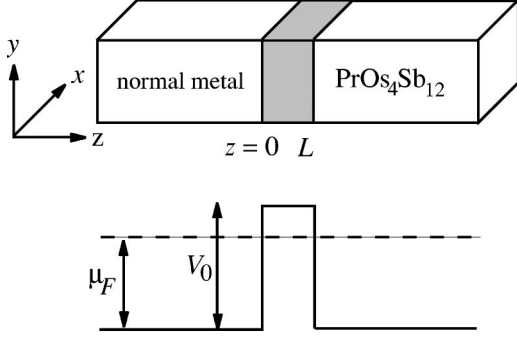
FIG. 1. The normal metal/POS junction is schematically illustrated.

tions are described by the Bogoliubov–de Gennes equation[45] and the conductance is calculated from the normal and the Andreev[46] reflection coefficients of junctions. We discuss candidates of pair potentials in anisotropic s wave symmetry for the spin-singlet pairing. The conductance is sensitive to the relation between the directions of currents and the position of point nodes. In some cases, shapes of the conductance deviate from those of the bulk DOS. In the spin-singlet pairing, we found that the conductance vanishes in the limit of the zero bias for most candidates. While in the spin-triplet pairing, we discuss the conductance for several candidates of pair potentials in the H and in L phases. The results show peak structures in the sub gap conductance for all candidates.

II. MODEL

We consider a junction between a normal metal (left hand side) and a POS (right hand side) as shown in Fig. 1. The geometry is chosen so that the current flows in the z direction. Periodic boundary conditions are assumed in the transverse directions to the current and the cross section of the junction is S.

The junction is described by the Bogoliubov-de Gennes (BdG) equation[45],

$$\int d\mathbf{r}' \begin{bmatrix} \delta(\mathbf{r}-\mathbf{r}')\hat{h}_0(\mathbf{r}') & \hat{\Delta}(\mathbf{r},\mathbf{r}') \\ -\hat{\Delta}^*(\mathbf{r},\mathbf{r}') & -\delta(\mathbf{r}-\mathbf{r}')\hat{h}_0^*(\mathbf{r}') \end{bmatrix} \begin{bmatrix} \hat{u}(\mathbf{r}') \\ \hat{v}(\mathbf{r}') \end{bmatrix}$$
$$= E \begin{bmatrix} \hat{u}(\mathbf{r}) \\ \hat{v}(\mathbf{r}) \end{bmatrix}, \tag{1}$$

$$\hat{h}_0(\mathbf{r}) = \left[-\frac{\hbar^2\nabla^2}{2m} - \mu_F + V(\mathbf{r}) \right] \hat{\sigma}_0. \tag{2}$$

In POS, the pair potential is expressed in the Fourier transformation

$$\hat{\Delta}(\mathbf{R},\mathbf{r}_r) = \frac{1}{\mathcal{V}} \sum_{\mathbf{k}} \hat{\Delta}(\mathbf{k}) e^{i\mathbf{k}\cdot\mathbf{r}_r}, \tag{3}$$

$$\hat{\Delta}(\mathbf{k}) = \begin{cases} i\mathbf{d}(\mathbf{k})\cdot\hat{\boldsymbol{\sigma}}\hat{\sigma}_2 & : \text{ triplet} \\ id(\mathbf{k})\hat{\sigma}_2 & : \text{ singlet}, \end{cases} \tag{4}$$

for $Z_c > L$, where L is the thickness of the insulator as shown in Fig. 1, $\mathbf{R} = (X_c, Y_c, Z_c) = (\mathbf{r}+\mathbf{r}')/2$, and $\mathbf{r}_r = \mathbf{r}-\mathbf{r}'$. The anisotropy of the pairing symmetry is characterized by $\hat{\Delta}(\mathbf{k})$ with $\mathbf{k} = (\mathbf{p},k_z)$ and $\mathbf{p} = (k_x,k_y)$. In normal metals and insulators, the pair potential is taken to be zero. The unit matrix and the Pauli matrices are denoted as $\hat{\sigma}_0$ and $\hat{\sigma}_j$ with $j = 1,2,3$, respectively. Throughout this paper, we measure the energy and the length in units of the Fermi energy $\mu_F = \hbar^2 k_F^2/2m$ and $1/k_F$, respectively. The potential of the insulator is given by

$$V(\mathbf{r}) = V_0[\Theta(z) - \Theta(z-L)], \tag{5}$$

and $q_z = k_F\sqrt{(V_0/\mu_F)-(k_z/k_F)^2}$ is the wave number in the z direction at the insulator. The Andreev and the normal reflection coefficients of the junction are calculated analytically

$$\hat{r}_{ee} = -z_0 z_1 [\hat{\sigma}_0 - \hat{W}][|z_1|^2 \hat{\sigma}_0 - z_0^2 \hat{W}]^{-1}, \tag{6}$$

$$\hat{r}_{he} = -e^{-i\varphi_s} 4\bar{k}_z^2 \bar{q}_z^{-2} \hat{\Delta}_{(+)}^{\dagger} \hat{R}_{(+)} [|z_1|^2 \hat{\sigma}_0 - z_0^2 \hat{W}]^{-1}, \tag{7}$$

$$\hat{R}_{(\pm)} = \frac{1}{2|\mathbf{q}_\pm|} \sum_{l=1}^{2} \left[\frac{K_{l,\pm}}{\Delta_{l,\pm}^2} \hat{P}_{l,\pm} \right], \tag{8}$$

$$\Delta_{l,\pm} = \sqrt{|\mathbf{d}_\pm|^2 - (-1)^l |\mathbf{q}_\pm|}, \tag{9}$$

$$K_{l,\pm} = \sqrt{E^2 - \Delta_{l,\pm}^2} - E, \tag{10}$$

$$\hat{P}_{l,\pm} = |\mathbf{q}_\pm|\hat{\sigma}_0 - (-1)^l \mathbf{q}_\pm \cdot \hat{\boldsymbol{\sigma}}, \tag{11}$$

$$\mathbf{q}_\pm = i\mathbf{d}_\pm \times \mathbf{d}_\pm^*, \tag{12}$$

$$\hat{W} = \hat{R}_{(-)} \hat{\Delta}_{(-)} \hat{\Delta}_{(+)}^{\dagger} \hat{R}_{(+)}, \tag{13}$$

$$z_0 = \frac{V_0}{\mu_F} \sinh(q_z L), \tag{14}$$

$$z_1 = (\bar{q}_z^2 - \bar{k}_z^2) \sinh(q_z L) + 2i\bar{k}_z \bar{q}_z \cosh(q_z L), \tag{15}$$

where φ_s is a macroscopic phase of superconductor, $\bar{k}_z = k_z/k_F$, $\bar{q}_z = q_z/k_F$, and $l(=1$ or $2)$ indicates the spin branch of a Cooper pair. These coefficients are characterized by the two Fourier components of the pair potentials

$$\hat{\Delta}_{(\pm)} = \begin{cases} id_\pm \hat{\sigma}_2 & : d_\pm \equiv d(\mathbf{p},\pm k_z): \text{ singlet} \\ i\mathbf{d}_\pm \cdot \hat{\boldsymbol{\sigma}}\hat{\sigma}_2 & : \mathbf{d}_\pm \equiv \mathbf{d}(\mathbf{p},\pm k_z): \text{ triplet}. \end{cases} \tag{16}$$

In unitary states, we find

$$\hat{R}_{(\pm)} = \frac{\sqrt{E^2 - |D_\pm|^2} - E}{|D_\pm|^2} \hat{\sigma}_0, \tag{17}$$

$$|D_\pm| = \begin{cases} |d_\pm| & : \text{ singlet} \\ |\mathbf{d}_\pm| & : \text{ triplet}. \end{cases} \tag{18}$$

The differential conductance is given by[47,48]

$$G_{NS}(E) = \frac{e^2}{h} N_c \int_0^{2\pi} d\phi \int_0^{\pi/2} d\theta \sin\theta$$

$$\times \mathrm{Tr}[\hat{\sigma}_0 - \hat{r}_{ee}\hat{r}_{ee}^\dagger + \hat{r}_{he}\hat{r}_{he}^\dagger]|_{E=eV_{\mathrm{bias}}}, \quad (19)$$

where $k_x = k_F \sin\theta\cos\phi$, $k_y = k_F \sin\theta\sin\phi$, $k_z = k_F \cos\theta$, $N_c = Sk_F^2/(2\pi)$ is the number of the propagating channels on the Fermi surface, and V_{bias} is the bias voltage applied to the junctions. The normal conductance of the junction is also calculated to be

$$G_N = \frac{2e^2}{h} N_c T_B, \quad (20)$$

$$T_B = \int_0^{2\pi} d\phi \int_0^{\pi/2} d\theta \sin\theta \frac{4\bar{k}_z^4 \bar{q}_z^4}{4\bar{k}_z^4 \bar{q}_z^4 + z_0^2}, \quad (21)$$

where T_B is the transmission probability of the junctions.

III. SPIN-SINGLET

Several candidates of pair potential are proposed theoretically for the spin-singlet superconductivity.[9,6] Here we show two sets of pair potentials discussed in Ref. 6,

$$d(H1) = \Delta_0 \frac{3}{2}(1 - \bar{k}_x^4 - \bar{k}_y^4 - \bar{k}_z^4), \quad (22)$$

$$d(L1) = \Delta_0(1 - \bar{k}_y^4 - \bar{k}_z^4), \quad (23)$$

$$d(H2) = \Delta_0(1 - \bar{k}_x^4 - \bar{k}_y^4), \quad (24)$$

$$d(L2) = \Delta_0(1 - \bar{k}_y^4), \quad (25)$$

where Δ_0 is the amplitude of the pair potential at the zero temperature, $\bar{k}_j = k_j/k_F$ for $j = x$, y and z are the normalized wave numbers on the isotropic Fermi surface. When the H phase is described by $d(H1)[d(H2)]$, the corresponding L phase is characterized by $d(L1)[d(L2)]$. In these pair potentials, anisotropic s wave symmetry is assumed to have a number of point nodes. In what follows, we define "node directions ($\mathbf{n}_{\mathrm{nd}}$)" in which the pair potential has point nodes. The pair potential of $d(H1)$, for instance, has six point nodes. The node directions are $(\bar{k}_x, \bar{k}_y, \bar{k}_z) = (\pm 1, 0, 0)$, $(0, \pm 1, 0)$, and $(0, 0, \pm 1)$. The thermal conductivity experiment indicates at least six point nodes in the H phase. In Fig. 2, we show the tunneling conductance of the pair potentials for $d(H1)$ and $d(L1)$ for several choices of Lk_F. Throughout this paper, we fix $V_0/\mu_F = 2.0$ and choose three values of Lk_F such as 0.0, 0.5, and 2.0. The transmission probability of junctions T_B are about 1.0, 0.4, and 0.003 for $Lk_F = 0.0$, 0.5 and 2.0, respectively. In what follows, the junction with $Lk_F = 2.0$ is refereed to as the low transparent junction or the junction with $T_B \ll 1$.

The results in Fig. 2(a) are the conductance for Eq. (22). In the limit of $T_B \ll 1$, the conductance shape is close to that of the bulk DOS denoted by a dot-dash line. Here the density of states are normalized by those of the normal state at the
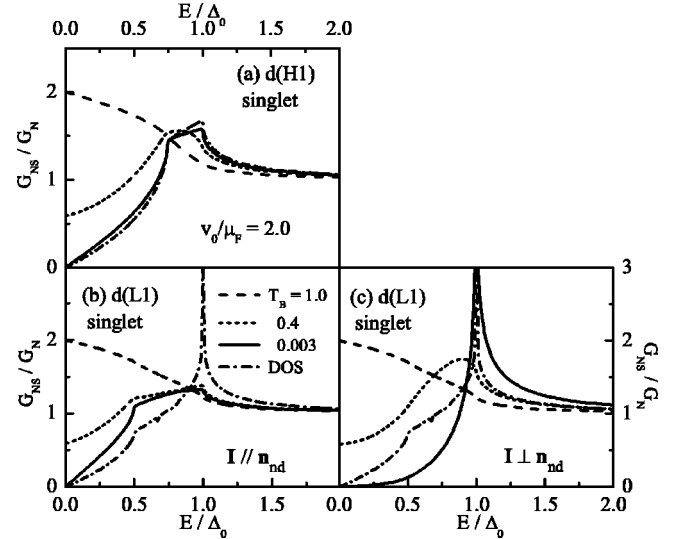

FIG. 2. The tunneling spectra of $d(H1)$ in (a) and those of $d(L1)$ in (b) and (c). In (b), the current is parallel to the node directions of $d(L1)$. In (c), the current is perpendicular to the node directions of $d(L1)$. The transmission probability of the junction in the normal states is denoted by T_B.

Fermi energy. When the pair potential are given in Eq. (23), the conductance depends on the current direction. In Fig. 2 (b), the current is parallel to the node direction of $d(L1)$ (i.e., $\mathbf{I}//\mathbf{n}_{\mathrm{nd}}$). The conductance shape in the limit of $T_B \ll 1$ becomes similar to that found in Fig. 2(a). When the current is perpendicular to the node direction (i.e., $\mathbf{I} \perp \mathbf{n}_{\mathrm{nd}}$), on the other hand, the large enhancement of the conductance is seen at $E = \Delta_0$ as shown in Fig. 2(c). Thus the tunneling spectra become anisotropic because of the anisotropy in the pair potential. The conductance shapes deviate from those of the bulk DOS even in the limit of $T_B \ll 1$ in both Figs. 2(b) and 2(c).

In Fig. 3, we show the tunneling spectra for Eqs. (24) and (25). The pair potential of $d(H2)$ is equivalent to $d(L1)$ under an appropriate rotation. Thus Figs. 3(a) and 3(b) are the same with Figs. 2(b) and 2(c), respectively. There are two point nodes in the direction of $(0, \pm 1, 0)$ in $d(L2)$.

In Figs. 3(c) and 3(d), the current is parallel and perpendicular to the node directions of $d(L2)$, respectively. In Fig. 3(d), there is a large peak at $E = \Delta_0$ and the subgap conductance has the same U shape as that of the bulk DOS. On the other hand in (c), the singularity at $E = \Delta_0$ is slightly suppressed and the sub gap conductance has a V shape. In Figs. 3(c) and 3(d), the anisotropy of the pair potential mainly appears in the shape of the sub gap conductance.

When the H phase is characterized by Eq. (22), an anisotropic $s + id$ wave pair potential in the L pahse was proposed by Goryo[9]

$$d(L3) = \Delta_0 \left[\frac{3}{2}(1 - \bar{k}_x^4 - \bar{k}_y^4 - \bar{k}_z^4) + i(\bar{k}_z^2 - \bar{k}_x^2) \right]. \quad (26)$$

In the second term, the d-wave component multiplied by i breaks the time-reversal symmetry. The pair potential in Eq. (26) has two point nodes on the Fermi surface in $(0, \pm 1, 0)$
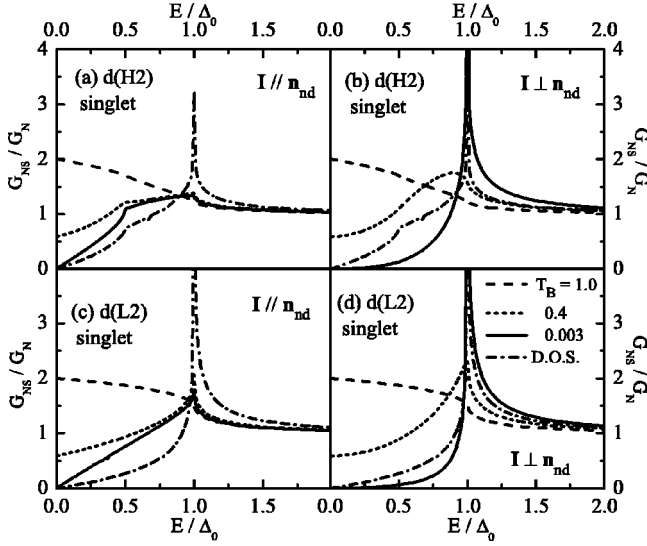
FIG. 3. The tunneling spectra of $d(H2)$ in (a) and (b) and those of $d(L2)$ in (c)–(d). In (a) and (c), the current is parallel to the node directions. In (b) and (d), the current is perpendicular to the node directions.

directions. In Fig. 4(a), we show the conductance for Eq. (26), where the current is perpendicular to the node direction. When the current is parallel to the node direction, the conductance is plotted in (b), where $\bar{k}_z^2 - \bar{k}_x^2$ in Eq. (26) is replaced by $\bar{k}_x^2 - \bar{k}_y^2$.

In both (a) and (b), the conductance in low transparent junctions has a peak around $E \sim \Delta_0$. The conductance in (a) is almost zero for $E < 0.75\Delta_0$ and are close to the bulk DOS for $E > 0.75\Delta_0$. On the other hand in (b), the conductance deviates from the bulk DOS even in the limit of $T_B \ll 1$ and has the V shape subgap structure. The anisotropy of the pair
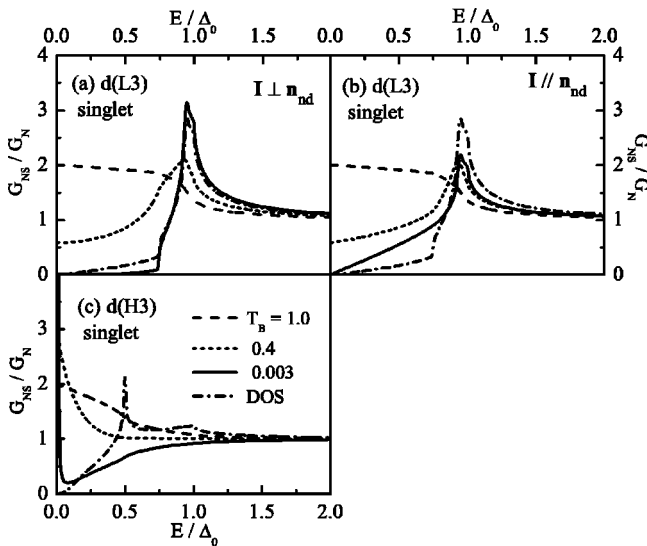

FIG. 4. The tunneling spectra of $d(L3)$ are shown in (a) and (b). The current is perpendicular to the node directions in (a). In (b), the current is perpendicular to the node directions. In (c), the conductance is plotted for $d(H3)$.
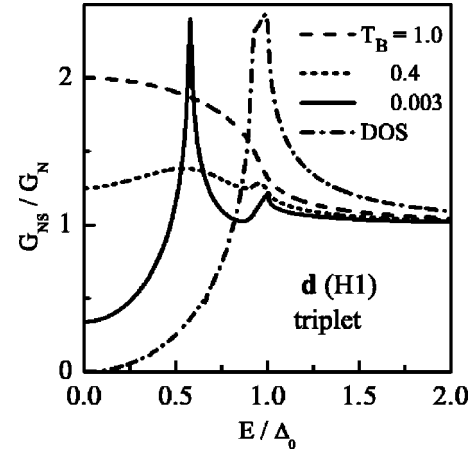

FIG. 5. The tunneling spectra of $\mathbf{d}(H1)$. The transmission probability of the junction in the normal states is denoted by T_B.

potential appears in the shape of the sub gap conductance as well as those in Figs. 3(c) and 3(d).

In addition to Eq. (22), it is possible to consider a pair potential with 6 point nodes by using gap functions of the cubic symmetry (O_h).[49] For example, a simple linear combination of three d wave gap functions

$$d(H3) = \Delta_0 (\bar{k}_x \bar{k}_y + \bar{k}_y \bar{k}_z + \bar{k}_z \bar{k}_x), \qquad (27)$$

has six point nodes. We show the conductance for $d(H3)$ in Fig. 4(c). The pair potential $d(H3)$ changes its sign on the Fermi surface, which is the most important difference between Eq. (27) and Eqs. (22)–(26). As a consequence, the conductance has the ZBCP as shown in Fig. 4(c) because a relation $d_+ \sim -d_-$ is approximately satisfied for $|\bar{k}_z| \sim 1$.

IV. SPIN-TRIPLET

As well as the spin-singlet superconductivity, a possibility of the spin-triplet superconductivity is also discussed in POS.[7] Ichioka *et al.* proposed a pair potential for the H phase[5]

$$\mathbf{d}(H1) = \Delta_0 \sqrt{\frac{27}{8}} (\bar{k}_x + i\bar{k}_y)(\bar{k}_y + i\bar{k}_z)(\bar{k}_z + i\bar{k}_x) \mathbf{e}_1, \quad (28)$$

where $\mathbf{e}_1$, $\mathbf{e}_2$ and $\mathbf{e}_3$ are three unit vectors in the spin space. Although Eq. (28) is not included in the gap functions of cubic symmetry (O_h), it explains 6 point nodes on the k_x, k_y, and k_z axes.

In Fig. 5, we show the conductance for the spin-triplet pair potentials in Eq. (28) for several choices of T_B. When the d vector has a single component, Eq. (13) becomes

$$\hat{W} = \frac{K_+ K_-}{|d_+||d_-|} e^{i\phi_- - i\phi_+} \hat{\sigma}_0, \qquad (29)$$

$$\mathbf{d}_\pm = \mathbf{e} |\mathbf{d}_\pm| e^{i\phi_\pm}, \qquad (30)$$

where $\mathbf{e}$ is a unit vector which points the direction of the d vector. In the case of $e^{i\phi_- - i\phi_+} = -1$, the ZBCP appears because of the ZES.[20] When $e^{i\phi_- - i\phi_+} = 1$, on the other hand, a
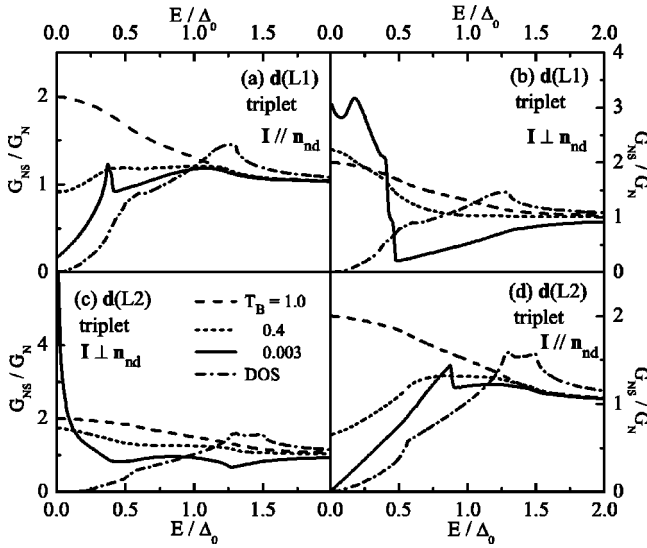
FIG. 6. The tunneling spectra of $\mathbf{d}(L1)$ in (a) and (b) and those of $\mathbf{d}(L2)$ in (c) and (d). The current flows in the node direction in (a) and (d). In (b) and (c), the node direction is perpendicular to the current.

peaklike structure is expected around $E = \Delta_0$. In Eq. (28), $e^{i\phi_- - i\phi_+}$ is a complex value because the pair potential breaks the time-reversal symmetry. In such a situation, the resonance energy deviates from both $E = 0$ and $E = \Delta_0$ and the resonance peak is expected between $E = 0$ and $E = \Delta_0$.[20] As a result, the conductance peak can be seen in the sub gap region as shown in Fig. 5. The bulk DOS vanishes at $E = 0$, whereas the conductance remains a finite value even in the limit of $T_B \ll 1$, which reflects the surface states due to the interference effect of a quasiparticle.

When the H phase is described by Eq. (28), corresponding pair potential in the L phase are given by

$$\mathbf{d}(L1) = \Delta_0 [(\bar{k}_x + i\bar{k}_y)(\bar{k}_y + i\bar{k}_z)(\bar{k}_z + i\bar{k}_x)\mathbf{e}_1 + \bar{k}_x \mathbf{e}_2],$$
(31)

or

$$\mathbf{d}(L2) = \Delta_0 [(\bar{k}_x + i\bar{k}_y)(\bar{k}_y + i\bar{k}_z)(\bar{k}_z + i\bar{k}_x)\mathbf{e}_1 + (\bar{k}_x + i\bar{k}_z)\mathbf{e}_2].$$
(32)

These pair potentials are in the nonunitary states. In the L phase, some of point nodes are removed by adding the p wave component to the d vector in Eq. (28). There are 4 and 2 point nodes in Eqs. (31) and (32), respectively. Since it is difficult to determine the relative amplitudes of $\mathbf{e}_1$ and $\mathbf{e}_2$ components, we simply add them with an equal amplitude. In Fig. 6, we show the conductance in these L phase pair potentials. When the current flows in the node direction of Eq. (31), the results are plotted in (a). The conductance for small T_B has a peak around $E = 0.3\Delta_0$ which may come from the large peak in Fig. 5. The DOS has a small peak at $E = 1.3\Delta_0$ which corresponds to the maximum value of $\Delta_{1,\pm}$ in Eq. (9). In (b), the current is perpendicular to the node direction of Eq. (31), where the $\mathbf{e}_2$ component in Eq. (31) is replaced by $\bar{k}_z \mathbf{e}_2$. The conductance for small T_B has a large amplitude around the zero bias. In spin-triplet super-

conductors, $\mathbf{d}_- = -\mathbf{d}_+$ represents the condition for the perfect formation of the ZES. Actually when $\mathbf{d}_+ = \mathbf{d} = \nu \mathbf{d}_-$ with $\nu = \pm 1$, the Andreev reflection probability becomes

$$R_A = \text{Tr} \hat{r}_{he} \hat{r}_{he}^\dagger = \sum_l \left| \frac{4\bar{k}^2 \bar{q}^2 \Delta_l K_l}{4\bar{k}^2 \bar{q}^2 \Delta_l^2 + z_0^2 (\Delta_l^2 - \nu K_l^2)} \right|^2.$$
(33)

In the limit of $E \to 0$ and $z_0 \gg 1$, this goes to

$$R_A = \begin{cases} 2 \left(\dfrac{4\bar{k}^2 \bar{q}^2}{2z_0^2} \right)^2 & : \quad \nu = 1, \\[3mm] 2 & : \quad \nu = -1, \end{cases}$$
(34)

where spin degree of freedom give rise to a factor 2. Thus the zero-bias conductance is independent of T_B when $\mathbf{d}_- = -\mathbf{d}_+$ is satisfied. The pair potential in (b) partially satisfies the condition because the $\mathbf{e}_2$ component is an odd function of k_z. As a consequence, the conductance at $E = 0$ increases with decreasing T_B as shown in (b). Thus the anisotropy of the pair potential in Eq. (31) appears the conductance shape around the zero bias. The conductance for Eq. (32) has a large peak as shown in (c), which is also explained by the ZES. On the other hand, the conductance linearly decreases with decreasing E in (d), where $(\bar{k}_x + i\bar{k}_z)\mathbf{e}_2$ in Eq. (32) is replaced by $(\bar{k}_y + i\bar{k}_x)\mathbf{e}_3$. A peak around $E = 0.8\Delta_0$ may come from the large subgap peak in Fig. 5. We note that the position of the subgap peaks may depends on parameters such as the thickness of the insulating layer and the relative amplitudes among the components in d vectors.

For the H phase, there are another candidates of the pair potentials such as[5]

$$\mathbf{d}(H2) = \Delta_0 [\bar{k}_x \mathbf{e}_1 + \bar{k}_y \epsilon \mathbf{e}_2 + \bar{k}_z \epsilon^2 \mathbf{e}_3],$$
(35)

$$\mathbf{d}(H3) = 2\Delta_0 [\bar{k}_x (\bar{k}_z^2 - \bar{k}_y^2)\mathbf{e}_1 + \bar{k}_y (\bar{k}_x^2 - \bar{k}_z^2)\mathbf{e}_2 + \bar{k}_z (\bar{k}_y^2 - \bar{k}_x^2)\mathbf{e}_3],$$
(36)

$$\mathbf{d}(H4) = 2\Delta_0 [\bar{k}_x (\bar{k}_z^2 - \bar{k}_y^2)\mathbf{e}_1 + \bar{k}_y (\bar{k}_x^2 - \bar{k}_z^2)\epsilon \mathbf{e}_2 + \bar{k}_z (\bar{k}_y^2 - \bar{k}_x^2)\epsilon^2 \mathbf{e}_3],$$
(37)

where $\epsilon = e^{i2\pi/3}$. The pair potential in Eq. (35) is similar to that of Barian-Werthamer (BW) states[50] described by

$$\mathbf{d}(BW) = \Delta_0 [\bar{k}_x \mathbf{e}_1 + \bar{k}_y \mathbf{e}_2 + \bar{k}_z \mathbf{e}_3].$$
(38)

Equation (35), however, is in the nonunitary states because of a phase factor. One spin branch has a full gap, other has eight point nodes in $(\pm 1, \pm 1, \pm 1)$ directions. The node directions of this pair potential contradict to the experimental results. In Fig. 7, we show the conductance for Eqs. (35) in (a). For comparison, we also show the conductance of the BW states in (b). The conductance for $T_B \ll 1$ increases rapidly with increasing E and has a peak around $E = 0.2\Delta_0$ as shown in (a). We note that the conductance spectra of the BW state in (b) also show a peak around $E = 0.5\Delta_0$. The peak structure may indicate some surface states of the BW type superconductors because the bulk DOS only have a peak at $E = \max(\Delta_{1,\pm}) = 1.4\Delta_0$ in (a) and $E = \Delta_0$ in (b).
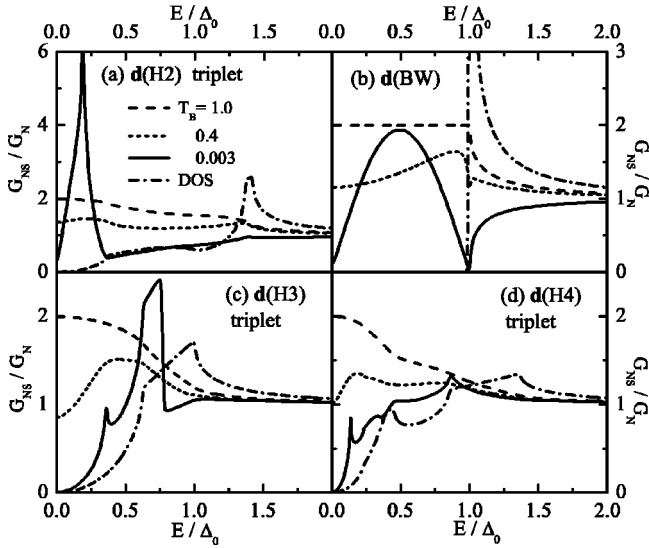
FIG. 7. The tunneling spectra of $\mathbf{d}(H2)$ in (a), $\mathbf{d}(H3)$ in (c), and $\mathbf{d}(H4)$ in (d). The conductance for BW states is shown in (b) for comparison.

FIG. 8. The tunneling spectra of $\mathbf{d}(\text{polar})$ in (a) and (b). Those for $\mathbf{d}(\text{ABM})$ are in (c) and (d).

When d vectors have more than two components, the shapes of the conductance spectra tend to have subgap peaks. Mathematically speaking, when $\mathbf{d}_-$ is not parallel to $\mathbf{d}_+^*$, the product of the two pair potentials in Eq. (13) becomes

$$\hat{\Delta}_{(-)}\hat{\Delta}_{(+)}^\dagger = \mathbf{d}_- \cdot \mathbf{d}_+^* \hat{\sigma}_0 + i\mathbf{d}_- \times \mathbf{d}_+^* \cdot \hat{\boldsymbol{\sigma}}. \tag{39}$$

The second term is a source of the sub gap peaks in the BW type states. At present, however, we have not yet confirmed an existence of some surface states. In Figs. 7(c) and 7(d), we show the conductance for Eqs. (36) and (37), respectively. There are 14 point nodes on the Fermi surface in Eqs. (36) and (37). Although the number of point nodes are larger than that found in the experiment, these pair potentials explain the six point nodes in k_x, k_y, and k_z directions. The conductance in Fig. 7(c) shows peak structures at $E = 0.36\Delta_0$ and $0.76\Delta_0$. These peaks are far from a peak in the bulk DOS at $E = \Delta_0$. The conductance in Fig. 7(d) also shows peak structures at $E = 0.13\Delta_0$, $0.34\Delta_0$ and $0.86\Delta_0$. However, there is no structure in the bulk DOS around the lowest peak. In addition to Eqs. (35)–(37), the polar state and the Anderson-Brinkman-Morel (ABM)[51] state are proposed for H phase of the spin-triplet pairing[7]

$$\mathbf{d}(\text{polar}) = \Delta_0 \bar{k}_z \mathbf{e}_3, \tag{40}$$

$$\mathbf{d}(\text{ABM}) = \Delta_0 (\bar{k}_x + i\bar{k}_y) \mathbf{e}_3. \tag{41}$$

The transition to L phase is caused by the spin-orbit coupling.[7] The polar state in Eq. (40) has a line node at $\bar{k}_z = 0$ and the ABM state in Eq. (41) has two point nodes at $\bar{k}_z = 1$. In Fig. 8 (a), we show the conductance in Eq. (40), where a plain including the line node, $k_z = 0$, is perpendicular to the current. The results show the ZBCP because Eq. (40) satisfies $\mathbf{d}_- = -\mathbf{d}_+$. In (b), we show the conductance in the ploar state, where $\bar{k}_z$ in Eq. (40) is replaced by $\bar{k}_x$ and a plain including the line node, $k_x = 0$, is parallel to the cur-
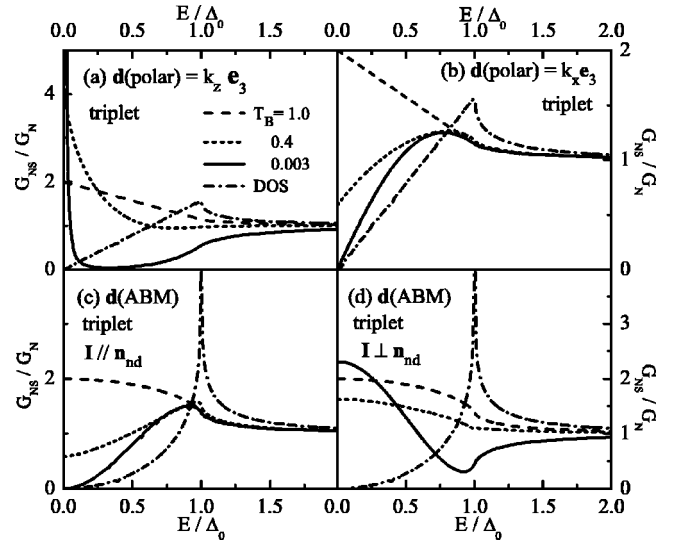
rent. The conductance at the zero-bias vanishes in the limit of $T_B \ll 1$ and increases linearly with increasing E. The shape of the conductance, however, deviates from that of the bulk DOS.

In Fig. 8(c), we show the conductance in Eq. (41), where the node direction is parallel to the current. In low transparent junctions, the conductance vanishes in the limit of $E \to 0$. The shape of the conductance, however, deviates from that of the bulk DOS. In (d), we show the conductance in the ABM state, where $\bar{k}_x + i\bar{k}_y$ in Eq. (41) is replaced by $\bar{k}_z + i\bar{k}_x$ and the node direction is perpendicular to the current. The broad ZBCP appears because Eq. (41) satisfies $\mathbf{d}_- = -\mathbf{d}_+$ only when $|\bar{k}_z| = 1$.[23] The height of the ZBCP is expected to be much larger in junctions with thicker insulating layers. The transmission probability for perpendicular injection to the thicker insulating layers become much larger than those for another incident angles. As a consequence, the condition $\mathbf{d}_- = -\mathbf{d}_+$ is better satisfied in junctions with thicker insulators.

In comparison with the spin-singlet pairing, the conductance in the spin-triplet superconductivity tends to have the subgap structures. The peak structures in Figs. 5, 6(a), and 6(d) are stemming from the broken time-reversal symmetry states in Eq. (28). The ZES is responsible for the peaks around the zero-bias in Figs. 6(b) and 6(c). The d vectors with multicomponents are the origin of the peaks in Fig. 7. Thus POS may be the spin-triplet superconductors if the subgap conductance shows complicated peak structures in experiments. The argument, however, is still a guess based on the calculated results. This is because it may be possible to consider another pair potentials with six point nodes.

In this paper, we do not consider the self-consistency of the pair potential near the junction interface. It is empirically known that the depletion of the pair potential modifies the conductance structure around $E = \Delta_0$ or maximum of $\Delta_{1,\pm}$. Our conclusions remain unchanged even in the self-

consistent pair potential unless the self-consistency does not change the symmetry of the pair potential and/or the number of components in d vectors.

V. CONCLUSION

We have discussed the differential conductance in normal-metal/insulator/POS junctions based on the Bogoliubov–de Gennes equation. For spin-singlet pairing, the conductance is calculated for three candidates of pair potentials in the anisotropic s wave symmetry. The results show that the conductance spectra depend strongly on the relation between the direction of currents and that of nodes. We found that the conductance vanishes in the limit of the zero bias and there is no anomalous behavior around the zero bias for these candidates. The conductance for $s+id$ wave symmetry in the L phase and that for d wave symmetry in the H phase are also demonstrated. In the case of spin-triplet superconductivity, we discuss the conductance for six candidates of pair potentials in the H phase and two candidates in the L phase. The results show peak structures in the subgap conductance for all candidates. The broken-time reversal symmetry states, the zero-energy states and d vectors with multi components arise these peak structures. POS may be a spin-triplet superconductor if the peak structures in the sub gap conductance is observed in future experiments. In particular, the presence or the absence of the ZBCP is an important information to address the pairing symmetry. Thus experiments of the tunneling spectra are desired.[52]

Recently, it has been pointed out that the magneto tunneling spectroscopy is a useful tool to know details of internal structures of pair potentials.[53] The tunnel spectra through a ferromagnetic tip[54] reflect the spin configuration of Cooper pairs in the case of the spin-triplet superconductors. Even in the spin-singlet superconductors, the absence of the time-reversal symmetry in ferromagnets affects the interference effects of a quasiparticle and modifies the tunneling spectra. At present, however, the investigations in this direction are limited in the d wave high-T_c superconductors. The magneto tunneling spectroscopy in another unconventional superconductors is a future problem.

In this paper, we assumed the clean ballistic junctions. It is known impurity scatterings in normal metals induce the proximity effect.[55] The proximity effect of unconventional superconductors with point nodes is also an open question.

---

*Electronic address: asano@eng.hokudai.ac.jp

[1] E. D. Bauer, N. A. Frederick, P.-C. Ho, V. S. Zapf, and M. B. Maple, Phys. Rev. B **65**, 100506(R) (2002).

[2] R. Vollmer, A. Faisst, C. Pfleiderer, H. v. Löhneysen, E. D. Bauer, P.-C. Ho, V. S. Zapf, and M. B. Maple, Phys. Rev. Lett. **90**, 057001 (2003).

[3] H. Kotegawa, M. Yogi, Y. Imamura, Y. Kawasaki, G. -q. Zheng, Y. Kitaoka, S. Ohsaki, H. Sugawara, Y. Aoki, and H. Sato, Phys. Rev. Lett. **90**, 027001 (2003).

[4] K. Izawa, Y. Nakajima, J. Goryo, Y. Matsuda, S. Osaki, H. Sugawara, H. Sato, P. Thalmeier, and K. Maki, Phys. Rev. Lett. **90**, 117001 (2003).

[5] M. Ichioka, N. Nakai, and K. Machida, J. Phys. Soc. Jpn. **72**, 1322 (2003).

[6] K. Maki, P. Thalmeier, Q. Yuan, K. Izawa, and Y. Matsuda, cond-mat/0212090 (unpublished).

[7] K. Miyake, H. Kohno, and H. Harima, J. Phys.: Condens. Matter **15**, L275 (2003).

[8] H. Sugawara, S. Osaki, S. R. Saha, Y. Aoki, H. Sato, Y. Inada, H. Shishido, R. Settai, Y. Onuki, H. Harima, and K. Oikawa, Phys. Rev. B **66**, 220504 (2002).

[9] J. Goryo, Phys. Rev. B **67**, 184511 (2003).

[10] Y. Tanaka and S. Kashiwaya, Phys. Rev. Lett. **74**, 3451 (1995).

[11] S. Kashiwaya and Y. Tanaka, Rep. Prog. Phys. **63**, 1641 (2000).

[12] J. Geerk, X. X. Xi, and G. Linker, Z. Phys. B: Condens. Matter **73**, 329 (1988); S. Kashiwaya, Y. Tanaka, M. Koyanagi, H. Takashima, and K. Kajimura, Phys. Rev. B **51**, 1350 (1995); L. Alff, H. Takashima, S. Kashiwaya, N. Terada, H. Ihara, Y. Tanaka, M. Koyanagi, and K. Kajimura, *ibid.* **55**, 14 757 (1997); M. Covington, M. Aprili, E. Paraoanu, L. H. Greene, F. Xu, J. Zhu, and C. A. Mirkin, Phys. Rev. Lett. **79**, 277 (1997); J. Y. T. Wei, N. -C. Yeh, D. F. Garrigus, and M. Strasik, *ibid.* **81**, 2542 (1998); I. Iguchi, W. Wang, M. Yamazaki, Y. Tanaka, and S. Kashiwaya, Phys. Rev. B **62**, R6131 (2000); H. Aubin, L. H. Greene, S. Jian, and D. G. Hinks, Phys. Rev. Lett. **89**, 177001 (2002); Z. Q. Mao, M. M. Rosario, K. D. Nelson, K. Wu, I. G. Deac, P. Schiffer, Y. Liu, T. He, K. A. Regan, and R. J. Cava, Phys. Rev. B **67**, 094502 (2003); A. Sharoni, O. Millo, A. Kohen, Y. Dagan, R. Beck, G. Deutscher, and G. Koren, *ibid.* **65**, 134526 (2002); A. Biswas, P. Fournier, M. M. Qazilbash, V. N. Smolyaninova, H. Balci, and R. L. Greene, Phys. Rev. Lett. **88**, 207004 (2002); Y. Dagan and G. Deutscher, *ibid.* **87**, 177004 (2001); J. W. Ekin, Y. Xu, S. Mao, T. Venkatesan, D. W. Face, M. Eddy, and S. A. Wolf, Phys. Rev. B **56**, 13 746 (1997).

[13] S. Kashiwaya, Y. Tanaka, M. Koyanagi, H. Takashima, and K. Kajimura, Phys. Rev. B **51**, 1350 (1995).

[14] S. Kashiwaya, Y. Tanaka, M. Koyanagi, and K. Kajimura, Phys. Rev. B **53**, 2667 (1996).

[15] Y. Tanaka and S. Kashiwaya, Phys. Rev. B **53**, 9371 (1996).

[16] Y. Tanuma, Y. Tanaka, M. Ogata, and S. Kashiwaya, J. Phys. Soc. Jpn. **67**, 1118 (1998); Y. Tanuma, Y. Tanaka, M. Ogata, and S. Kashiwaya, Phys. Rev. B **60**, 9817 (1999); Y. Tanuma, Y. Tanaka, and S. Kashiwaya, *ibid.* **64**, 214519 (2001).

[17] M. Fogelström, D. Rainer, and J. A. Sauls, Phys. Rev. Lett. **79**, 281 (1997); D. Rainer, H. Burkhardt, M. Fogelström, and J. A. Sauls, J. Phys. Chem. Solids **59**, 2040 (1998).

[18] M. Matsumoto and H. Shiba, J. Phys. Soc. Jpn. **64**, 1703 (1995).

[19] C. R. Hu, Phys. Rev. Lett. **72**, 1526 (1994).

[20] Y. Asano, Y. Tanaka, and S. Kashiwaya, cond-mat/0307345.

[21] L. J. Buchholtz and G. Zwicknagl, Phys. Rev. B **23**, 5788 (1981).

[22] F. Laube, G. Goll, H. v. Löhneysen, M. Fogelström, and F. Lichtenberg, Phys. Rev. Lett. **84**, 1595 (2000); Z. Q. Mao, K. D. Nelson, R. Jin, Y. Liu, and Y. Maeno, *ibid.* **87**, 037003 (2001); Ch. Wälti, H. R. Ott, Z. Fisk, and J. L. Smith, *ibid.* **84**, 5616 (2000).

[23] M. Yamashiro, Y. Tanaka, and S. Kashiwaya, Phys. Rev. B **56**, 7847 (1997); M. Yamashiro, Y. Tanaka, Y. Tanuma, and S. Kashiwaya, J. Phys. Soc. Jpn. **67**, 3224 (1998); M. Yamashiro,

Y. Tanaka, and S. Kashiwaya, *ibid.* **67**, 3364 (1998); M. Yamashiro, Y. Tanaka, Y. Tanuma, and S. Kashiwaya, *ibid.* **68**, 2019 (1999).

[24] C. Honerkamp and M. Sigrist, Prog. Theor. Phys. **100**, 53 (1998); C. Honerkamp and M. Sigrist, J. Low Temp. Phys. **111**, 895 (1998).

[25] Y. Tanuma, K. Kuroki, Y. Tanaka, and S. Kashiwaya, Phys. Rev. B **64**, 214510 (2001); K. Sengupta, I. Žutić, H.-J. Kwon, V. M. Yakovenko, and S. Das Sarma, *ibid.* **63**, 144531 (2001).

[26] Y. Tanaka, T. Asai, N. Yoshida, J. Inoue, and S. Kashiwaya, Phys. Rev. B **61**, R11 902 (2000).

[27] Y. Tanaka, T. Hirai, K. Kusakabe, and S. Kashiwaya, Phys. Rev. B **60**, 6308 (1999); T. Hirai, K. Kusakabe, and Y. Tanaka, Physica C **336**, 107 (2000); K. Kusakabe and Y. Tanaka, *ibid.* **367**, 123 (2002); K. Kusakabe and Y. Tanaka, J. Phys. Chem. Solids **63**, 1511 (2002).

[28] N. Stefanakis, Phys. Rev. B **64**, 224502 (2001); Z. C. Dong, D. Y. Xing, and J. Dong, *ibid.* **65**, 214512 (2002); Z. C. Dong, D. Y. Xing, Z. D. Wang, Z. Zheng, and J. Dong, *ibid.* **63**, 144520 (2001); Yu. S. Barash, M. S. Kalenkov, and J. Kurkijarvi, *ibid.* **62**, 6665 (2000); M. H. S. Amin, A. N. Omelyanchouk, and A. M. Zagoskin, *ibid.* **63**, 212502 (2001); S.-T. Wu and C.-Y. Mou, *ibid.* **66**, 012512 (2002).

[29] Y. Asano and Y. Tanaka, Phys. Rev. B **65**, 064522 (2002).

[30] Y. Asano, Y. Tanaka, and S. Kashiwaya, cond-mat/0302287 (unpublished).

[31] Y. Tanaka and S. Kashiwaya, Phys. Rev. B **53**, R11 957 (1996).

[32] Y. Tanaka and S. Kashiwaya, Phys. Rev. B **56**, 892 (1997).

[33] Y. Tanaka and S. Kashiwaya, Phys. Rev. B **58**, 2948 (1998).

[34] Y. Tanaka and S. Kashiwaya, J. Phys. Soc. Jpn. **68**, 3485 (1999).

[35] Y. Tanaka and S. Kashiwaya, J. Phys. Soc. Jpn. **69**, 1152 (2000).

[36] Y. S. Barash, H. Burkhardt, and D. Rainer, Phys. Rev. Lett. **77**, 4070 (1996).

[37] E. Il'ichev, V. Zakosarenko, R. P. J. IJsselsteijn, V. Schultze, H.-G. Meyer, H. E. Hoenig, H. Hilgenkamp, and J. Mannhart, Phys. Rev. Lett. **81**, 894 (1998).

[38] E. Il'ichev, M. Grajcar, R. Hlubina, R. P. J. IJsselsteijn, H. E. Hoenig, H. -G. Meyer, A. Golubov, M. H. S. Amin, A. M. Zagoskin, A. N. Omelyanchouk, and M. Yu. Kupriyanov, Phys. Rev. Lett. **86**, 5369 (2001).

[39] Y. Asano, Phys. Rev. B **63**, 052512 (2001).

[40] Y. Asano, Phys. Rev. B **64**, 014511 (2001).

[41] Y. Asano, Phys. Rev. B **64**, 224515 (2001).

[42] Y. Asano, J. Phys. Soc. Jpn. **71**, 905 (2002); Y. Asano, Physica C **367**, 92 (2002); **367**, 157 (2002).

[43] Y. Asano and K. Katabuchi, J. Phys. Soc. Jpn. **71**, 1974 (2002).

[44] Y. Asano, Y. Tanaka, M. Sigrist, and S. Kashiwaya, Phys. Rev. B **67**, 184505 (2003).

[45] P. G. de Gennes, *Superconductivity of Metals and Alloys* (Benjamin, New York, 1966).

[46] A. F. Andreev, Zh. Éksp. Theor. Fiz, **46**, 1823 (1964) [Sov. Phys. JETP **19**, 1228 (1964)].

[47] G. E. Blonder, M. Tinkham, and T. M. Klapwijk, Phys. Rev. B **25**, 4515 (1982).

[48] Y. Takane and H. Ebisawa, J. Phys. Soc. Jpn. **61**, 1685 (1992).

[49] M. Sigrist and K. Ueda, Rev. Mod. Phys. **63**, 239 (1991).

[50] R. Balian and N. R. Werthamer, Phys. Rev. **131**, 1553 (1963).

[51] P. W. Anderson and P. Morel, Phys. Rev. **123**, 1911 (1961).

[52] After submission, a tunneling experiment was reported by H. Suderow, S. Vieria, J. D. Strand, S. Bud'ko, and P. C. Canfield, cond-mat/0306463 (unpublished). The results show the U-shape subgap structure for the *L* phase.

[53] Y. Tanuma, K. Kuroki, Y. Tanaka, R. Arita, S. Kashiwaya, and H. Aoki, Phys. Rev. B **66**, 094507 (2002); Y. Tanuma, Y. Tanaka, K. Kuroki, and S. Kashiwaya, *ibid.* **66**, 174502 (2002); Y. Tanaka, H. Tsuchiura, Y. Tanuma, and S. Kashiwaya, J. Phys. Soc. Jpn. **71**, 271 (2002); Y. Tanaka, Y. Tanuma, K. Kuroki, and S. Kashiwaya, *ibid.* **71**, 2102 (2002); Y. Tanaka, H. Itoh, H. Tsuchiura, Y. Tanuma, J. Inoue, and S. Kashiwya, *ibid.* **71**, 2005 (2002).

[54] J.-X. Zhu, B. Friedman, and C. S. Ting, Phys. Rev. B **59**, 9558 (1999); S. Kashiwaya, Y. Tanaka, N. Yoshida, and M. R. Beasley, *ibid.* **60**, 3572 (1999); I. Zutic and O. T. Valls, *ibid.* **60**, 6320 (1999); N. Yoshida, Y. Tanaka, J. Inoue, and S. Kashiwaya, J. Phys. Soc. Jpn. **68**, 1071 (1999); T. Hirai, N. Yoshida, Y. Tanaka, J. Inoue, and S. Kashiwaya, *ibid.* **70**, 1885 (2001); N. Yoshida, H. Itoh, T. Hirai, Y. Tanaka, J. Inoue, and S. Kashiwaya, Physica C **367**, 135 (2002); T. Hirai, Y. Tanaka, N. Yoshida, Y. Asano, J. Inoue, and S. Kashiwaya, Phys. Rev. B **67**, 174501 (2003); Y. Tanuma, Y. Tanaka, K. Kuroki, and S. Kashiwaya, *ibid.* **66**, 174502 (2002); N. Yoshida, Y. Asano, H. Itoh, Y. Tanaka, and J. Inoue, J. Phys. Soc. Jpn. **72**, 895 (2003).

[55] Y. Tanuma, Y. Tanaka, M. Yamashiro, and S. Kashiwaya, Phys. Rev. B **57**, 7997 (1998); Y. Tanaka, Y. Tanuma, and S. Kashiwaya, *ibid.* **64**, 054510 (2001); Y. Tanaka, Yu. V. Nazarov, and S. Kashiwaya, Phys. Rev. Lett. **90**, 167003 (2003); A. A. Golubov and M. Y. Kupriyanov, Pis'ma Zh. Éksp. Teor. Fiz. **69**, 242 (1999) [JETP Lett. **69**, 262 (1999)]; **67**, 478 (1998) [**67**, 501 (1998)]; A. Poenicke, Yu. S. Barash, C. Bruder, and V. Istyukov, Phys. Rev. B **59**, 7102 (1999); K. Yamada, Y. Nagato, S. Higashitani, and K. Nagai, J. Phys. Soc. Jpn. **65**, 1540 (1996); T. Lück, U. Eckern, and A. Shelankov, Phys. Rev. B **63**, 064510 (2002); N. Kitaura, H. Itoh, Y. Asano, Y. Tanaka, J. Inoue, Y. Tanuma, and S. Kashiwaya, J. Phys. Soc. Jpn. **72**, 1718 (2003).